

# Probing the tensor structure of lattice three-gluon vertex in Landau gauge

Milan Vujanović<sup>1</sup> and Tereza Mendes<sup>1</sup>

<sup>1</sup>*Instituto de Física de São Carlos, Universidade de São Paulo, Caixa Postal 369, 13560-970 São Carlos, SP, Brasil*

In this paper we test an approximate method that is often used in lattice studies of the Landau gauge three-gluon vertex. The approximation consists in describing the lattice correlator with tensor bases from the continuum theory. With the help of vertex reconstruction, we show that this “continuum” approach may lead, for general kinematics, to significant errors in vertex tensor representations. Such errors are highly unwelcome, as they can lead to wrong quantitative estimates for vertex form factors and related quantities of interest, like the three-gluon running coupling. As a possible solution, we demonstrate numerically and analytically that there exist special kinematic configurations for which the vertex tensor structures can be described exactly on the lattice. For these kinematics, the dimensionless tensor elements are equal to the continuum ones, regardless of the details of the lattice implementation. We ran our simulations for an  $SU(2)$  gauge theory in two and three spacetime dimensions, with Wilson and  $\mathcal{O}(a^2)$  tree-level improved gauge actions. Our results and conclusions can be straightforwardly generalised to higher dimensions and, with some precautions, to other lattice correlators, like the ghost-gluon, quark-gluon and four-gluon vertices.

## I. INTRODUCTION

The primitively divergent vertex functions of quantum chromodynamics (QCD) and its quenched version, the pure Yang-Mills theory, have been the subject of numerous non-perturbative investigations in the past two decades. There are two main reasons why these objects attract considerable interest among researchers. Firstly, by studying the vertices, and in particular their infrared (IR) properties, one might be able to learn something about confinement. Of particular interest in this regard are the Gribov-Zwanziger [1–4] and Kugo-Ojima [5] confinement scenarios, and their relation to the IR behaviour of the ghost and gluon propagators. The second reason to study the vertex functions has to do with the functional bound state calculations, for which these quantities constitute a key component, see [6–12] for examples.

The non-perturbative methods that have been used to study the vertices can roughly be divided into two main categories. The first includes functional techniques like the Dyson-Schwinger equations (DSEs) [13–16], functional renormalisation group (FRG) [17], and others. The second consists of various lattice formulations and the corresponding Monte Carlo (MC) simulations, see [18] and references therein. Both of these groups of approaches have their particular strengths and weaknesses. In the case of lattice investigations, there is an issue related to the tensor representations of lattice vertices, which we would like to address in detail in this paper.

In most lattice studies of 3-point vertices, authors use the corresponding tensor elements from the continuum theory [19–27]. However, due to the breaking of rotational symmetry, the continuum tensor bases cannot be applied in discretised spacetime, at least not for general kinematics. This has been explicitly demonstrated for the lattice gluon propagator in Landau gauge [28]. There are a few reasons why this practice persists, despite the errors that it might induce on calculated vertex form factors. One is that, for most vertex functions, the correct alternative to using a continuum basis is simply unknown, despite some clues from lattice perturbation theory [29]. The other important justification is that some lattice studies are almost exclusively interested in the infrared region [25, 26], where discretisation effects are expected to be small and can arguably be ignored. As an alternative to continuum bases, some authors have used tree-level tensor elements from lattice perturbation theory [30–33], which however do not provide a complete representation for most vertex functions.

In this paper, we attempt to put these matters on a firmer footing, in terms of discretisation error estimates. We present a simple method, based on vertex reconstruction, that enables one to quantify how (un)well some basis describes a given correlation function. We apply the method to the lattice Landau gauge gluon propagator and three-gluon vertex, and demonstrate that, for general kinematics, these functions are described relatively poorly by the continuum tensor bases. However, we also show numerically that there exist special kinematic configurations for which these functions can be described, with virtually no errors, in terms of continuum basis elements. We demonstrate analytically why this last statement holds, and argue that it is also applicable, with some caveats, to other QCD correlators. The possibility to describe the tensor structure of a given lattice correlator with virtually no discretisation artifacts is of particular interest for lattice studies of the QCD running coupling [20, 21, 24, 34–37], where elimination of uncertainties in the ultraviolet energy region is of paramount importance.

The paper is organised as follows. In Section II we provide details of our lattice setup. In Section III we describe the reconstruction procedure, and test the method by using it on the Landau gauge lattice gluon propagator. In Section IV we employ the reconstruction approach to probe the tensor elements of the Landau gauge three-gluon vertex, and comment on our findings. Some further discussions, indirectly related to the results presented here, as well as conclusions are provided in Section V. The important technical details have been relegated to the two appendices.

## II. NUMERICAL SETUP

### A. Generation of configurations

In this work we will consider a lattice  $SU(2)$  gauge theory in two and three dimensions, with periodic boundary conditions and an equal number of points  $N$  in all directions. The gauge field configurations used in our simulations have been generated with the standard gauge action of Wilson [38], as well as with an  $\mathcal{O}(a^2)$  tree-level improved theory [39–43]. Denoting the Wilson and improved gauge actions as  $S_W$  and  $S_I$ , respectively, one has

$$\begin{aligned}
 S_W &= \frac{\beta}{N_c} \sum_{\text{plaq}} \text{Re} [\text{Tr} (\mathbb{1} - U_{\text{plaq}})] , \\
 S_I &= \frac{5\beta}{3N_c} \sum_{\text{plaq}} \text{Re} [\text{Tr} (\mathbb{1} - U_{\text{plaq}})] - \frac{\beta}{12N_c} \sum_{\text{rect}} \text{Re} [\text{Tr} (\mathbb{1} - U_{\text{rect}})] ,
 \end{aligned}
 \tag{1}$$

where  $N_c = 2$ ,  $U_{\text{plaq}}$  is a Wilson plaquette operator, and  $U_{\text{rect}}$  stands for  $1 \times 2$  and  $2 \times 1$  rectangle operators. More explicitly, we have

$$\begin{aligned}
 U_{\text{plaq}}(x) &= U_\mu(x) U_\nu(x + \hat{\mu}) U_\mu^\dagger(x + \hat{\nu}) U_\nu^\dagger(x) , \\
 U_{\text{rect}}(x) &= U_\mu(x) U_\nu(x + \hat{\mu}) U_\nu(x + \hat{\nu} + \hat{\mu}) U_\mu^\dagger(x + 2\hat{\nu}) U_\nu^\dagger(x + \hat{\nu}) U_\nu^\dagger(x) + \\
 &\quad U_\mu(x) U_\mu(x + \hat{\mu}) U_\nu(x + 2\hat{\mu}) U_\mu^\dagger(x + \hat{\mu} + \hat{\nu}) U_\mu^\dagger(x + \hat{\nu}) U_\nu^\dagger(x) .
 \end{aligned}
 \tag{2}$$

In (2), all of the links  $U_\sigma$  are elements of an  $SU(2)$  gauge group. They are parametrised as  $U \equiv U_0 \mathbb{1} + i \vec{U} \cdot \vec{\sigma}$ , where  $\mathbb{1}$  is the identity matrix and  $\vec{\sigma} \equiv (\sigma^1, \sigma^2, \sigma^3)$  are the Pauli matrices. The coefficients  $(U_0, \vec{U})$  are real numbers, and one has  $U_0^2 + \vec{U}^2 = 1$ . The gauge actions of (1) formally become equivalent to the continuum Yang-Mills theory in the limit  $a \rightarrow 0$ , if one defines the lattice coupling as  $\beta \equiv 4/(a^2 g^2)$  (in 2D), or  $\beta \equiv 4/(a g^2)$  (in 3D). Here,  $g$  is a bare coupling constant.

For configuration updates, we used a multi-hit variant of the Metropolis algorithm, with 12 hits (update suggestions) per one staple evaluation. Parameters of the algorithm were tuned such that, on average, approximately half of all suggested updates was accepted. Starting from a cold configuration, we performed 5000 update steps for thermalisation, for all the volumes and  $\beta$  values considered in this work. Upon thermalisation, we kept all of the subsequent configurations for measurements, 2400 for each  $(N, \beta)$  pair, and performed an integrated autocorrelation time analysis when calculating statistical uncertainties. For an estimation of the integrated autocorrelation time  $\tau_{\text{int}}$ , we used an automatic windowing procedure outlined in section 3.3 of [44], with parameter  $S = 2.5$ . For the quantities studied in sections III and IV of this paper, the biggest obtained  $\tau_{\text{int}}$  was slightly larger than 1 (recall that  $\tau_{\text{int}} = 0.5$  implies there are no autocorrelations).

Comparisons of Wilson and  $\mathcal{O}(a^2)$  improved setups were done at constant physics, i. e. for each  $\beta$  used in the Wilson approach, we tried to find a corresponding value in the improved theory, such that the lattice spacings are roughly the same (in physical units) for the two cases. To determine the spacing  $a$  in physical units, the measurements of the static quark-antiquark potential were used. The scale was set via the string tension, with the value  $\sqrt{\sigma} = 0.44$  GeV. To improve the signal quality for the potential, we used APE smearing [45]: the associated parameter values are collected in Table I. In case of the Wilson gauge action, we also compared the dimensionless quantity  $\sqrt{\sigma} a$  from our simulations with the analytic result of [46] (for 2D theory), as well as with a fit of equation (67) from [47] (for 3D theory). In all cases we obtained reasonable agreement of results, see Table I for details.

## B. Gluon potential and gauge fixing

We use a standard linear definition for the lattice gluon potential  $A_\mu$ , which is an element of the  $SU(2)$  Lie algebra:

$$A_\mu(x) \equiv \frac{1}{2} [U_\mu(x) - U_\mu^\dagger(x)] = i \vec{U}_\mu(x) \cdot \vec{\sigma}. \quad (3)$$

The colour components of  $A_\mu(x)$  are obtained as

$$A_\mu^b(x) \equiv \frac{1}{2i} \text{Tr} [A_\mu(x) \sigma^b], \quad b = 1 \dots 3. \quad (4)$$

The correlation functions in which we are interested are gauge-dependent, and to evaluate them we fix the thermalised configurations  $\{U\}$  to Landau gauge. The details on how this is done can be found in [48–50]. More precisely, we use equation (3.3) of [49], with an expansion to leading order in  $\alpha$ , and subsequent reunitarisation. The free parameter  $\alpha$  can be tuned to improve convergence, and its optimal values are collected for each set of considered gauge field configurations in Table I. We are using this so-called Cornell method to fix the gauge due to the algorithm's straightforward implementation in a parallel environment. The iterative gauge-fixing process is stopped when the convergence criterion

$$\frac{1}{V} \sum_x \sum_{b=1}^3 [\nabla \cdot A(x)]_b^2 \leq 10^{-14}, \quad (5)$$

is satisfied. In the above expression,  $V \equiv a^d N^d$  is the lattice volume and  $\nabla \cdot A_\mu^b(x)$  stands for the colour components of the lattice divergence of  $A_\mu$ . More precisely, one has

$$\nabla \cdot A_\mu^b(x) \equiv \sum_{\mu=1}^d [A_\mu^b(x) - A_\mu^b(x - e_\mu)]. \quad (6)$$

With (5) one approximates, in terms of lattice quantities, the continuum Landau gauge condition  $\partial_\mu A_\mu(x) = 0$ . With the gauge-fixing criterion thus specified, we can turn to the final ingredient needed for the evaluation of  $n$ -point gluon correlators in momentum space, which is the Fourier transform of  $A_\mu^b(x)$ . It is defined as

$$\begin{aligned} \tilde{A}_\mu^b(k) &\equiv \sum_x A_\mu^b(x) \exp[2\pi i(k \cdot x + k_\mu/2)], \quad \text{with} \\ k_\mu &\equiv \frac{2\pi n_\mu}{aN}, \quad n_\mu \in [0, N-1]. \end{aligned} \quad (7)$$

In (7), the  $k_\mu/2$  modification is applied in order to recover the continuum Landau gauge condition with  $\mathcal{O}(a^2)$  corrections, instead of  $\mathcal{O}(a)$  ones [20]. Namely, with the lattice divergence of (6), and the Fourier transform  $\tilde{A}_\mu^b(k)$  as defined in (7), the lattice version of the momentum space Landau gauge condition takes the form

$$\sum_{\mu=1}^d \hat{p}_\mu \tilde{A}_\mu^b(p) = 0, \quad (8)$$

where  $\hat{p}_\mu = 2 \sin(p_\mu/2)$ . The above relation is formally equivalent to  $p_\mu \tilde{A}_\mu^b(p) = 0$  up to order  $\mathcal{O}(a^2)$ . In actual simulations the number on the r. h. s. of (8) will not be exactly 0, but will have some value on the order of  $10^{-6}$  or  $10^{-7}$ , as dictated by the gauge-fixing criterion (5).

## III. VERTEX RECONSTRUCTION AND LATTICE GLUON PROPAGATOR

We wish to test the applicability of describing the lattice correlators, primarily the three-gluon vertex, with continuum tensor bases. A question arises as to how can this be done in practical terms, i. e. how does one can check if some basis is suitable for a description of a given vertex function. One approach is presented in

[28], where it was applied to the Landau gauge lattice gluon propagator. The technique employed there can be useful, but it only works for vertices with a single tensor element. Here we propose a method based on vertex reconstruction, which can (in principle) be used for arbitrary correlators. For the gluon propagator, our approach reduces to the same steps used in [28].

We denote a generic lattice correlation function with  $\Gamma_\mu(p)$ , where the superindex  $\mu$  stands for any applicable Lorentz indices, and  $p$  subsumes the independent momentum variables. We wish to test if  $\Gamma_\mu(p)$  can be described with a basis  $\tau_\mu^j(p)$ , with index  $j$  denoting individual tensor elements. That is, we wish to see if the relation

$$\Gamma_\mu(p) = \sum_j \mathcal{F}^j(p) \tau_\mu^j(p), \quad (9)$$

holds, with  $\mathcal{F}^j$  being a dressing/coefficient function (or form factor) of a tensor element  $\tau_\mu^j$ . One way to do this is to attempt a vertex reconstruction. Explicitly, one constructs the projectors for the basis  $\tau_\mu$ , and projects out the functions  $\mathcal{F}$  from the lattice vertex  $\Gamma_\mu$ . One then reconstructs the correlator, via (9), from the dressings  $\mathcal{F}$  and the  $\tau_\mu$  basis. Finally, one compares the reconstructed and the original vertex. If the relation (9) is correct, then no information will be lost when computing the  $\mathcal{F}$  functions. Consequently, the reconstructed vertex will be equal to the original one. Any discrepancy between the reconstructed and original vertex points to an inadequacy of the basis  $\tau_\mu$ , and the “size” of the discrepancy is an indication on how unsuitable the basis is, for given kinematics. Let us test these ideas on the gluon. The continuum, infinite-volume version of the Landau gauge gluon is given by

$$D_{\mu\nu,p}^{\text{cont},ab} = \left( \delta_{\mu\nu} - \frac{p_\mu p_\nu}{p^2} \right) \delta^{ab} D(p^2), \quad (10)$$

with colour indices  $a, b$ . On the lattice, one can deduce the tensor structure of the Landau gauge gluon by combining the propagators definition with (8). The lattice gluon propagator is given by

$$D_{\mu\nu}^{ab}(p) = \frac{1}{V} \left\langle \tilde{A}_\mu^a(p) \tilde{A}_\nu^b(-p) \right\rangle, \quad (11)$$

with  $V$  the lattice volume and  $\tilde{A}(p)$  defined in (7). From the constraint of (8) and the definition of (11), one can straightforwardly show that the lattice gluon propagator in Landau gauge has the form (up to corrections dictated by numerical gauge-fixing):

$$D_{\mu\nu}^{ab}(p) = \left( \delta_{\mu\nu} - \frac{\hat{p}_\mu \hat{p}_\nu}{\hat{p}^2} \right) \delta^{ab} D(p^2). \quad (12)$$

The structure of (12) will remain the same regardless of the employed lattice action, as long as the same gauge-fixing algorithm is used for all simulations. We assume the propagator to be diagonal in colour space, as shown above, and will henceforth consider the colour-averaged quantities  $D_{\mu\nu} \equiv \frac{1}{3} \sum_a D_{\mu\nu}^{aa}$ . This leaves only the tensorial part. For both the representation of (10), and the one of (12), the form factor  $D(p)$  can be projected out with a simple  $D$ -dimensional Kronecker tensor  $\delta_{\mu\nu}$ . In other words, one has

$$D(p) = \frac{1}{\mathcal{N}} \delta_{\mu\nu} D_{\mu\nu}(p), \quad (13)$$

with implied summation over repeated indices. For  $p = 0$ , the normalisation factor  $\mathcal{N}$  equals  $D$  (the number of dimensions), otherwise it is  $D - 1$  [20]. Since the projector of (13) is momentum-independent, the discussion of tensor structure is actually superfluous for the Landau gauge gluon propagator. Put differently, a detailed consideration of the propagators tensor representation has no bearing on the way that one calculates the form factor  $D(p)$ . Nevertheless, taking a closer look at this two-point function is useful for demonstrating the basic ideas of our method.

For the reconstruction part of our approach, we take the propagator dressing of (13), and obtain the reconstructed correlator by plugging in  $D(p)$  into either of equations (10) or (12). The end result is then compared to the original propagator, i.e.  $D_{\mu\nu}^{\text{calc}} \sim \tilde{A}_\mu \tilde{A}_\nu$ . Since we do not wish to compare the two-point

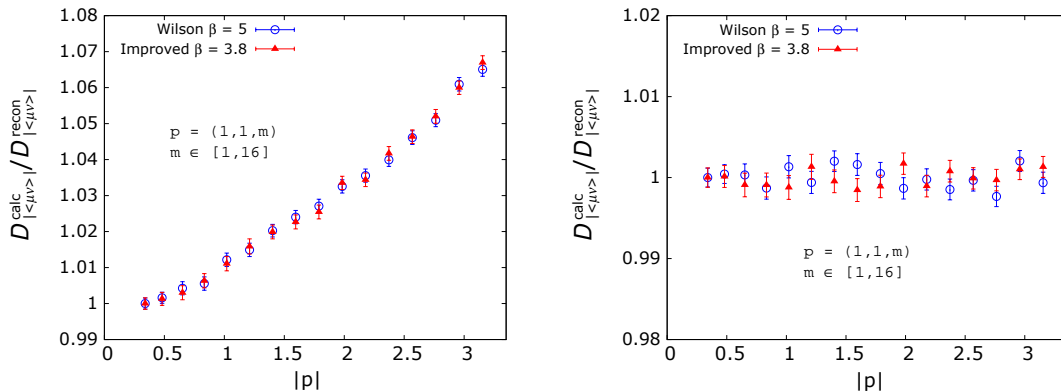


Figure 1. Comparison of calculated and reconstructed gluon on a  $32^3$  lattice, for near-axis momentum  $p$  and with  $|p| \equiv \sqrt{p^2}$ . Results are in lattice units, with  $p$  given in terms of components of vector  $n_\mu$  of (7). *Left*: Propagator reconstruction according to (10). *Right*: Reconstruction according to (12). Shown are data for Wilson and  $\mathcal{O}(a^2)$  improved actions.

functions for each individual value of indices  $\mu$  and  $\nu$ , we will consider the index-averaged quantities, namely

$$\frac{D_{|\langle\mu\nu\rangle|}^{\text{calc}}}{D_{|\langle\mu\nu\rangle|}^{\text{recon}}} \equiv \frac{\sum_\mu \sum_\nu |D_{\mu\nu}^{\text{calc}}|}{\sum_\mu \sum_\nu |D_{\mu\nu}^{\text{recon}}|}, \quad (14)$$

with  $|\cdot|$  denoting a (complex number) absolute value. When evaluating the ratios like the one above, we will always use the absolute value of propagators and vertices. There are multiple reasons for this, and here we mention two of them. Firstly, for diagonal momenta (i. e.  $p_\mu = p_\nu$  for all  $\mu, \nu$ ), performing an index average for the reconstructed Landau gauge correlators would always yield zero, without the absolute value. For the gluon propagator, this can be seen by taking an ordinary (no absolute value) index average of the r. h. s. of either of equations (10) or (12), for diagonal momenta. The second reason is that the signal quality is generally better for absolute value of correlators than the correlators themselves. We discuss the second point in more detail at the end of section IV B. To confirm that the index-averaging procedure does not introduce a large bias for the results, we've also performed calculations where propagators were compared component-wise (e. g.  $D_{11}^{\text{calc}}/D_{11}^{\text{recon}}$ , etc.), and checked that such comparisons yield (on average) results similar to the ratio of (14). The biggest relative difference in results between the two methods was on the order of one percent.

A remark is in order regarding our notation. In equation (14),  $D_{\mu\nu}^{\text{calc}}$  does **not** stand for a Monte Carlo average, akin to the one of (11). It instead denotes a product of vector potentials, considered for each gauge field configuration separately. The same goes for the reconstructed gluon and the whole ratio in (14): the ratios are evaluated on the level of individual configurations, and in the end these results are averaged to get the final estimate, together with the associated uncertainty. For better statistics, we also perform averages over permutations of momentum components, of which there are 2 in two dimensions, and 6 in three dimensions<sup>1</sup>. Due to hypercubic symmetry (a symmetry under permutations and reflections of coordinates), the dressing function  $D(p)$  of (13) should remain unchanged when components of  $p$  are interchanged, thus justifying the aforementioned permutation average. The final results for momenta near the lattice axis in a 3D theory are given in Figure 1. In Fig. 1 we do not consider the momenta exactly along the axis, in order to avoid finite volume effects, see the first data point of Fig. 2.

The plots in Fig. 1 show the behaviour that one would expect, based on our previous discussions. The data indicate that the reconstruction method works for the gluon propagator. To get more valuable insight, one can use the continuum tensor of (10) for reconstruction, but for diagonal momenta. The result is given in Fig. 2, and it suggests that along the lattice diagonal, one can describe the lattice gluon with a continuum tensor structure. The explanation for this is straightforward. For diagonal kinematics, the non-trivial part of

<sup>1</sup> As an example of permutations in 3D, one may look at a momentum  $p$  with components  $p = (a, b, c)$ . To each result for  $p$  we add results for permuted versions, i. e. for momenta  $p' = (a, c, b)$ ,  $p'' = (b, a, c)$ , and three others, and make an average of this sum.

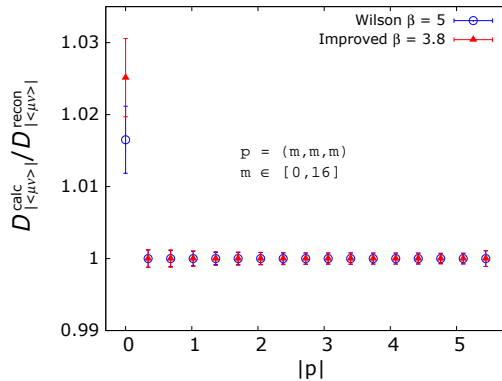


Figure 2. Comparison of calculated and reconstructed gluon on a  $32^3$  lattice, for diagonal momentum  $p$  and with reconstruction according to (10). Results are in lattice units, with  $p$  given in terms of components of vector  $n_\mu$  of (7).  $|p|$  stands for  $\sqrt{p^2}$ .

the transverse projector  $T_{\mu\nu}^p = \delta_{\mu\nu} - p_\mu p_\nu / p^2$  [bracketed object on the r. h. s. of equations (10) and (12)] is momentum-independent. To be more explicit, with  $p^\mu = p^\nu$  (for all  $\mu, \nu$ ), one gets<sup>2</sup>

$$\frac{p_\mu p_\nu}{p^2} = \frac{\hat{p}_\mu \hat{p}_\nu}{\hat{p}^2} = \frac{1}{D}, \quad \text{for all } \mu, \nu, \quad (15)$$

where  $D$  is the number of dimensions. The above statement is discretisation-independent, meaning that the exact form of  $\hat{p}_\mu$ , and the details of the lattice formulation, are unimportant. As we show later, for the three-gluon vertex there are several kinematic configurations for which the same observation holds. Regarding the results in Fig. 2, we additionally point out that the discrepancy at  $p = 0$  is most likely due to finite-volume artifacts, see section II of [28] for a more detailed discussion. Some other effects that might also contribute at zero momentum are discussed in Section V.

Before moving further, we wish to address the absence, in Figures 1 and 2, of any appreciable differences between data for the Wilson action gluon and the  $\mathcal{O}(a^2)$  improved one. Two main factors contribute to this result. First, in our plots we consider the ratios of propagators, where the correlator dressing function  $D(p^2)$  (which is different for the two kinds of lattice gauge action) should drop out. Second, the gauge field configurations coming from both  $S_W$  and  $S_I$  actions, have been numerically subjected to the constraint of (8), which ensures that the two kinds of propagator have an identical tensor structure given in (12).

## IV. THE THREE-GLUON VERTEX

### A. Colour and tensor structure in the continuum

The lattice three-gluon vertex is defined as

$$\Gamma_{\mu\nu\rho}^{abc}(p, q, r) = \frac{1}{V} \left\langle \tilde{A}_\mu^a(p) \tilde{A}_\nu^b(q) \tilde{A}_\rho^c(r) \right\rangle, \quad (16)$$

where  $r = -(p + q)$ . Actually, the above quantity is not the one-particle-irreducible (1PI) vertex, but simply a gluon three-point function: to obtain the true 1PI vertex, one needs to amputate the gluon legs, see e. g. [19]. For most of our results, this distinction is unimportant, as we will be looking at vertex ratios where the gluon propagators coming from the amputation would anyway drop out. Before presenting our results for the function of (16), we need briefly to discuss its colour and tensor decomposition in the continuum. Let us start with the

<sup>2</sup> We are grateful to Attilio Cucchieri for pointing this out to us.

colour part. In general, the continuum three-gluon vertex has the form (we temporarily suppress the momentum dependencies):

$$\Gamma_{\mu\nu\rho}^{abc} = f^{abc} \Gamma_{\mu\nu\rho}^a + d^{abc} \Gamma_{\mu\nu\rho}^s, \quad (17)$$

with  $f^{abc}$  and  $d^{abc}$  the antisymmetric and symmetric structure constants, respectively.  $\Gamma_{\mu\nu\rho}^{a/s}$  are the corresponding tensor elements. Orthogonality of the colour constants (i. e.  $f^{abc}d^{abc} = 0$ ) can be used to project out the desired tensor piece. When doing vertex reconstruction, the colour symmetric and antisymmetric parts can be analysed independently of each other. For the  $SU(2)$  group which we are considering, these matters are simpler since  $d^{abc} = 0$ . It is also possible that for other gauge groups, like  $SU(3)$ , the symmetric contributions to the vertex are negligibly small. Results that might point to this conclusion can be found in [21, 52–56]. In either case, we extract the tensor part of the correlator with a contraction  $\Gamma_{\mu\nu\rho} = f^{abc} \Gamma_{\mu\nu\rho}^{abc}$ , where  $\Gamma_{\mu\nu\rho}^{abc}$  is given in (16).

This brings us to the tensor part. For covariant gauges and a number of dimensions greater than 2, the three-gluon vertex can be decomposed into 14 linearly independent tensor elements. For Landau gauge with more than 2 spacetime dimensions, the number of elements is reduced to 4, due to transversality conditions. In our numerics we mostly employ the transverse orthonormal (ON) basis, used for the first time in [57]. That paper gives a full account on how the basis is constructed, but we repeat the main steps in our Appendix A 1 as well. In the same Appendix we prove, using the ON basis, that in two dimensions a single tensor element is adequate to describe the Landau gauge three-gluon vertex. Summing up, for our study in three dimensions we use the decomposition

$$\Gamma_{\mu\nu\sigma}(p, q, r) = \sum_{j=1}^4 \mathcal{B}^j(p, q, r) \rho_{\mu\nu\sigma}^j(p, q, r), \quad (18)$$

with elements  $\rho_{\mu\nu\sigma}^j$  given in equation (A11) of [57], as well as in equation (A11) of our Appendix A 1. In two dimensions, only the tensor  $\rho_{\mu\nu\sigma}^2$  is needed to represent the three-gluon coupling, as all the other ones vanish. Since the basis  $\rho_{\mu\nu\sigma}^j$  is orthonormal, it is straightforward to get the corresponding form factors from the calculated vertex. Namely, one has

$$B^j(p, q, r) = \rho_{\mu\nu\sigma}^j(p, q, r) \cdot \Gamma_{\mu\nu\sigma}(p, q, r), \quad j = 1 \dots 4. \quad (19)$$

Henceforth, we employ the Einstein summation convention, unless stated otherwise. The ON basis is useful for numerics and vertex reconstruction, but it is not very “friendly” for certain analytic manipulations. We are mainly referring to our intent to demonstrate, for the three-gluon correlator, some results akin to equation (15) for the gluon. Such relations can be proved with the ON basis as well, but for calculations of this type we prefer to use another tensor decomposition for the vertex, where some arguments become more transparent and simple. We refer to the said decomposition as the “Simple” one, and show the construction of corresponding elements in Appendix A 2. The connection between the ON and Simple basis is also provided in the Appendix.

## B. Vertex results in two dimensions

The setup of our calculations for the three-gluon coupling is an extension of the procedure we outlined for the gluon propagator. The lattice vertex is calculated as a product  $\Gamma_{\mu\nu\rho}^{abc} \sim \tilde{A}_\mu^a \tilde{A}_\nu^b \tilde{A}_\rho^c$ , and its colour dependence is taken care of with the  $f^{abc}$  projection. We attempt to reconstruct the remaining tensor piece with appropriate tensor bases, and form the ratios of index-averaged quantities. The index average of (say) a calculated vertex is defined as

$$\Gamma_{|\langle\mu\nu\rho\rangle|}^{\text{calc}} = \sum_{\mu\nu\rho} |\Gamma_{\mu\nu\rho}^{\text{calc}}|, \quad (20)$$

where  $|\cdot|$  again denotes a complex number absolute value. As in the case of the gluon propagator, the values for vertex ratios are obtained for each gauge field configuration separately, and these results are averaged over to obtain the final answer and the corresponding error estimate. As noted in the previous section, in a two-dimensional theory only the tensor element  $\rho_{\mu\nu\sigma}^2$  of (A11) is required for a reconstruction in the continuum.

Owing to momentum conservation,  $r = -(p + q)$ , only two out of three momenta that enter the three-gluon vertex are independent. In our simulations we take these vectors to be  $p$  and  $q$ . For improved statistics we

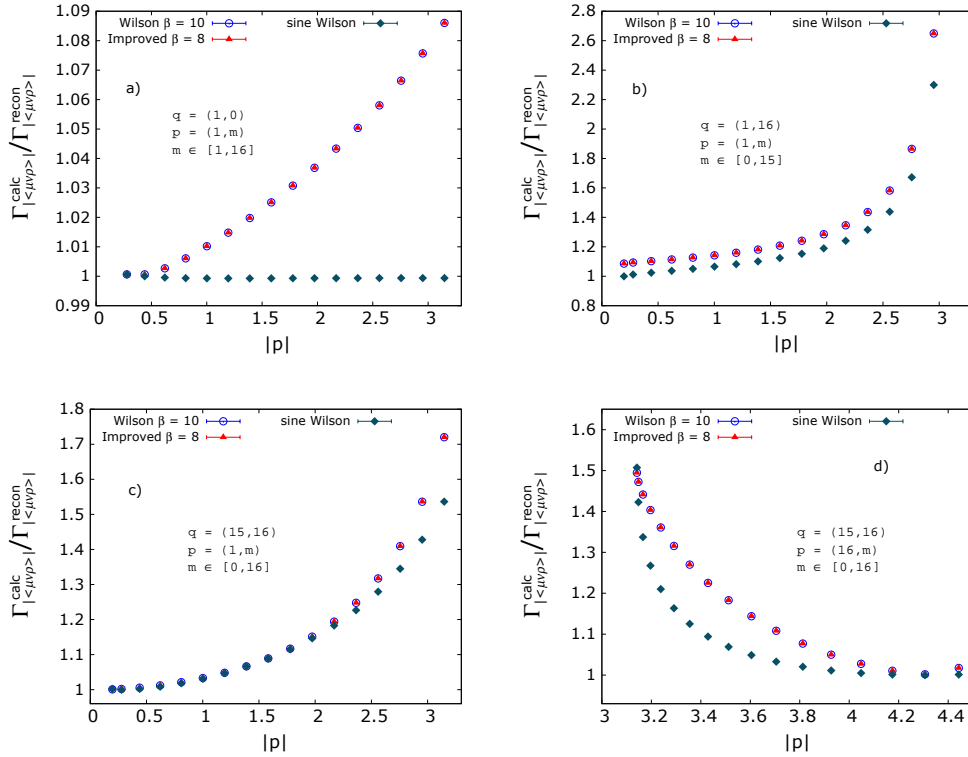


Figure 3. Ratios of calculated and reconstructed vertices on a  $32^2$  lattice, as functions of  $|p| = \sqrt{p^2}$ . Reconstruction was done with the ON basis tensor  $\rho_{\mu\nu\sigma}^2$  of (A11). “Sine” data are for a reconstruction with modified momenta  $(\hat{p}, \hat{q})$ , where e.g.  $\hat{p} = 2 \sin(p/2)$ . Results are in lattice units, with all momenta given in terms of components of vector  $n_\mu$  of (7). See text for further discussion.

perform permutation averages, wherein to each result for momenta  $(p, q)$  we add results where components of  $p$  and  $q$  have been permuted in various ways. We do not consider such permutations for each momentum  $p$  and  $q$  separately, but instead perform the same transformation on both vectors. Thus, as in the case of the gluon propagator, we average over a total of 2 permutations in 2D, and 6 permutations in 3D.

One final notion we need to introduce before discussing the results is that of the “sine improvement”. From Landau gauge condition (8) and the definition of lattice three-gluon vertex (16), it is clear that this correlator should satisfy (up to corrections from numerical gauge-fixing):

$$\hat{p}_\mu \hat{q}_\nu \hat{r}_\rho \Gamma_{\mu\nu\rho}(p, q, r) = 0. \quad (21)$$

The continuum Landau gauge vertex obeys the same relation as above, but with  $(\hat{p}, \hat{q}, \hat{r})$  replaced with  $(p, q, r)$ . The analogy suggests that, to describe the tensor structure of the lattice correlator, one needs to use modified momenta, like  $p \rightarrow \hat{p} = 2 \sin(p/2)$ , when constructing the vertex tensor elements. However, for general kinematics, the sine modification cannot be carried out for all three momenta at once, since it would spoil the momentum conservation condition  $r = -(p + q)$  [since in general  $\sin(x + y) \neq \sin(x) + \sin(y)$ ]. We still want to test if the sine correction can help with the reduction of errors. Aside from a normal reconstruction with independent momenta  $(p, q)$ , we also consider a sine-modified method, where vectors  $(\hat{p}, \hat{q})$  are used for the tensor elements. In our plots, we refer to the second procedure as “sine”. We will only display the sine results for Wilson gauge action, to prevent the graphs from getting too cluttered. An approach similar to our sine correction was already used for the lattice measurements of the three-gluon running coupling [21].

This brings us to the results. In Fig. 3 we show the plots of our data for several kinematic configurations on a two-dimensional lattice. In the first plot, the vector  $q$  has relatively small components. Consequently, the sine improvement can be applied to all momenta, while approximately keeping the momentum conservation intact, i.e.  $\hat{r} \approx -(\hat{p} + \hat{q})$ . This is why the sine-adjusted reconstruction works well in the whole examined range of  $p$

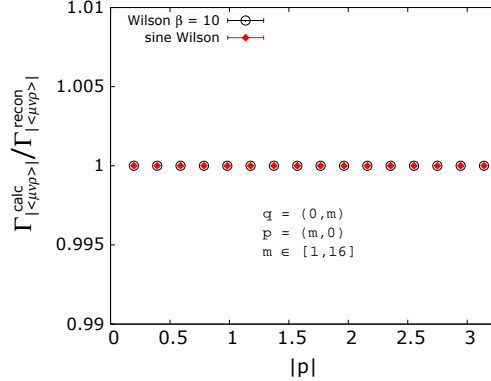


Figure 4. Results of vertex reconstruction on a  $32^2$  lattice, for a quasi-symmetric momentum configuration  $(p^2, q^2, r^2) = (s^2, s^2, 2s^2)$ . Reconstruction was done with an ON basis tensor  $\rho_{\mu\nu\sigma}^2$  of (A11). Results are in lattice units, with all momenta given in terms of components of vector  $n_\mu$  of (7).  $|p|$  stands for  $\sqrt{p^2}$ , and “sine” data refers to reconstruction with momenta  $(\hat{p}, \hat{q})$ , where e. g.  $\hat{p} = 2 \sin(p/2)$ . See text for further discussion.

values. In contrast, in the second plot in the Figure, one of the  $q$  components is large, and neither of the two reconstruction methods describes well the lattice correlator for the entire considered range of  $p$  momentum.

The third and fourth plot of Fig. 3 demonstrate the influence of proximity to the diagonal kinematic configuration. In the third plot, this influence can be seen on the left side of the graph, and in the fourth, on the right. The results indicate that, just as for the gluon propagator, close to the lattice diagonal one can represent the lattice three-gluon vertex with a continuum tensor basis. Also evident from these graphs is the positive effect of the sine modification, which always mitigates the discretisation errors. Note that two of the graphs in Fig. 3 are missing a data point corresponding to the case  $p = q$ . The reason is that for such kinematics, the reconstructed Landau gauge three-gluon vertex is equal to zero. We show analytically why this happens in Appendix B 2.

So far we’ve encountered two examples of kinematics where the errors in vertex tensor elements are virtually vanishing: these are the situation with one vertex momentum being small (with the adjustment  $(p, q) \rightarrow (\hat{p}, \hat{q})$ ), and the kinematics close to the diagonal. We now look at another sample of special kinematics, given by

$$p = (s, 0), \quad q = (0, s), \quad (22)$$

where  $s \equiv 2\pi n/(aN)$ , with integer  $n \in [1, N - 1]$ . We refer to the above configuration as quasi-symmetric, since one has  $(p^2, q^2, r^2) = (s^2, s^2, 2s^2)$ . A fully symmetric situation is not possible on a lattice, in less than three dimensions. Nonetheless, the quasi-symmetric configuration has some interesting features of its own. First, the sine modification can be applied to all momenta without affecting the momentum conservation, i. e.  $\hat{r} = -\hat{p} - \hat{q}$ . One can thus make a basis that manifestly satisfies (21), and that should describe exactly the lattice correlator. This can be seen in Fig. 4, where the reconstruction with sine momenta gives back the full vertex. Another important characteristic of quasi-symmetric kinematics, also visible in the plot, is that no sine correction is actually needed: an ordinary continuum basis works equally well. In Appendix B 1 we discuss this analytically, showing how the continuum tensors can describe the lattice correlator in certain situations. There we also comment on the applicability of these ideas to other QCD vertices.

Before moving on, we want to comment on the signal quality in our calculations. Most of our graphs have rather small error bars, with some uncertainties even being too small to be noticed on the overall scale of the plot. This has to do with our use of the absolute value for propagators and vertices. As already stated, we determine all the quantities on the level of individual field configurations, and average over these results to obtain the final estimate. With this kind of setup, use of the absolute value enhances the signal quality. We show this in Fig. 5, where we give a Monte Carlo average of a vertex component  $\Gamma_{121}$ , with and without the absolute value. For a calculation without  $|\cdot|$ , we consider only the imaginary part of the vertex, as the real part has a value of zero within (admittedly large) error bars. The reason that the absolute value makes such a difference should be fairly obvious: while in a standard calculation there are both negative and positive contributions to vertices, the absolute value makes all the contributions to Monte Carlo averages strictly non-negative.

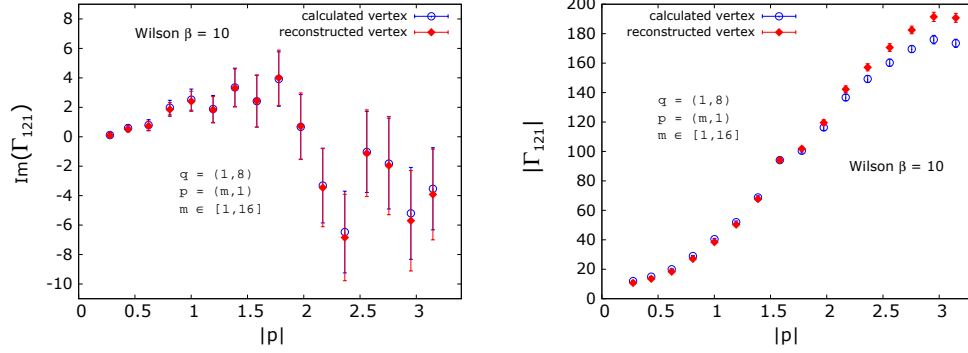


Figure 5. *Left*: Monte Carlo (MC) average of an imaginary part of vertex component  $\Gamma_{121}$ , on a  $32^2$  lattice. *Right*: MC average of an absolute value of  $\Gamma_{121}$ . Results are in lattice units, with momenta given in terms of vector  $n_\mu$  of (7). Reconstructed and calculated vertex agree at the graph mid-point due to special kinematics, see Fig. 4.

### C. Vertex results in three dimensions

In Figure 6 we present the results of our simulations for certain three-dimensional kinematic configurations. We point out a big difference between the data shown in the upper and lower panel of the Figure. The behaviour of the vertex ratios in the first two graphs agrees nicely with some of our preceding arguments, but this is not the

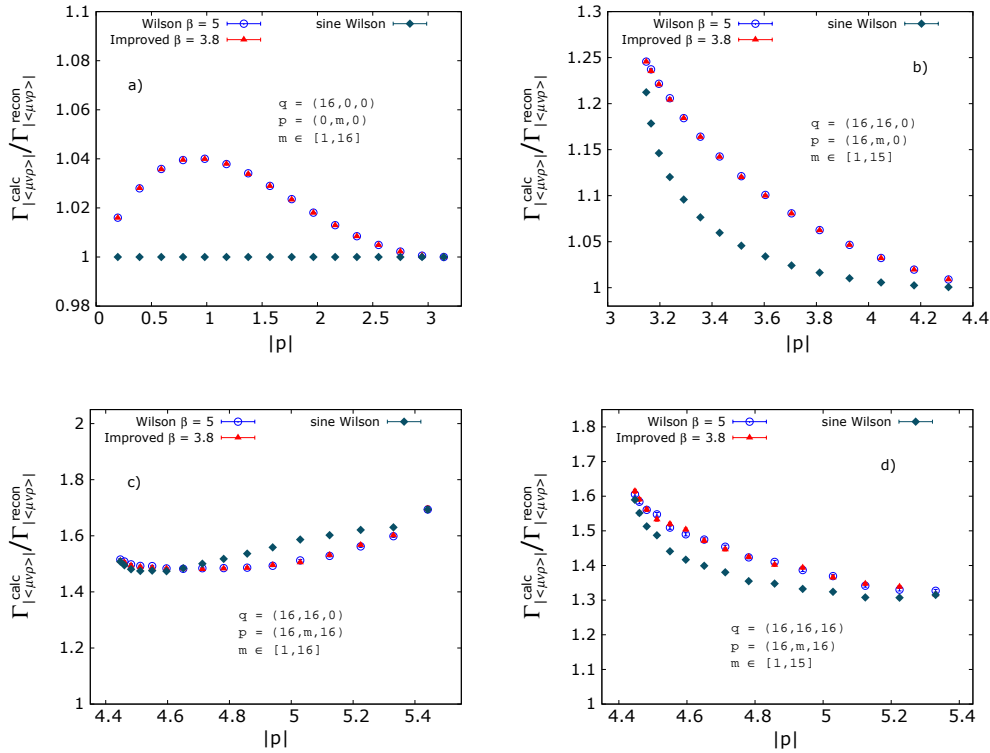


Figure 6. Vertex ratios for certain kinematics a  $32^3$  lattice, as functions of  $|p| = \sqrt{p^2}$ . Reconstruction was done with ON tensor elements of (A11). Results are in lattice units, with momenta given in terms of vector  $n_\mu$  of (7). “Sine” data refers to reconstruction with momenta  $(\hat{p}, \hat{q})$ , where e. g.  $\hat{p} = 2 \sin(p/2)$ . See text for further discussion.

case in the last two plots. For instance, due to the proximity of diagonal kinematics, the ratio in the last graph should evolve to a number very close to unity, as  $p$  increases. Instead, it gets stuck at values of about 1.3, even for momentum points very close to the lattice diagonal. Either there is something wrong with our claim that diagonal kinematic configurations are special in terms of vertex tensor representations, or the reconstruction method gives incorrect results in certain situations. We will now argue for the second case.

When considering vertex tensor parametrisations, like the one in equation (18), one usually thinks of the form factors (e.g.  $\mathcal{B}_j$ ) as having definite values, for fixed kinematics. But in Monte Carlo simulations, the evaluation of these functions can be plagued by large uncertainties: for some three-gluon examples, see [26, 31, 33], or the left panel of our Fig. 5. Since the form factors can be quite noisy in some cases, it stands to reason to expect that the reconstruction procedure that involves these objects can give unpredictable results. In two dimensions, this was not an issue since there was a single tensor element/form factor involved, and (as shown in Fig. 5), the absolute value practically eliminates the fluctuations in that function. But in a three-dimensional space, with up to four tensors being involved, a calculation with strictly non-negative quantities cannot help with the fact that these tensor elements, and their corresponding form factors, can combine to give vertex estimates which are simply wrong.

The above assumption about statistical noise does not explain the difference in “quality” between the upper and lower panels of Figure 6. Both sets of data required the same tensor basis of four elements for reconstruction, and according to our preceding hypothesis one would expect to see the same qualitative behaviour in all the plots. For this issue, there is a straightforward explanation in terms of kinematics. For configurations examined in the first two plots of Figure 6, the tensor structure  $\rho_{\mu\nu\sigma}^2$  (the only non-vanishing one in 2D) dominates over all the other elements of equation (A11), rendering the calculation essentially two-dimensional. These matters are explored in more detail at the end of section A 1.

We’ve run several tests to check if the discrepancies seen in some of our 3D data are caused by systematic errors in our calculations. To test the correctness of the employed tensor basis, for kinematics in Fig. 6, we’ve successfully reconstructed several different test functions which have the same symmetries and quantum numbers as the (continuum) three-gluon vertex. For a check on our 3D lattice codes for the generation of configurations and gauge-fixing, we reproduced the  $\beta = 5$ ,  $V = 32^3$  gluon data of [58]. As an additional test, we came up with another method for demonstrating the special status of certain kinematic configurations, in terms of vertex tensor representations.

The second method consists in calculating directly the contraction of (21), both with standard momenta  $(p, q)$  and with their sine-transformed versions. One looks for kinematics where the number ‘0’ on the r. h. s of (21) is numerically of the same order of magnitude for both sets of vectors. An advantage of this technique, compared to vertex reconstruction, is that it avoids the possible issues with noisy vertex form factors, but the procedure also has limitations in its range of applicability. The contraction approach cannot be used to identify the special kinematic configurations for (say) ghost-gluon and quark-gluon vertex, since the tensor structures of those functions are not determined solely by gauge-fixing and equations like (21). In Figure 7 we give the results

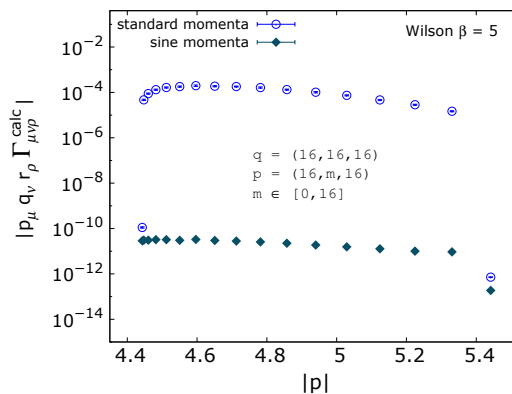


Figure 7. Absolute value of contraction (21), for particular kinematics on a  $32^3$  lattice. The contraction was calculated with standard discretised momenta  $(p, q)$ , and with their sine versions  $(\hat{p}, \hat{q})$ , where e.g.  $\hat{p} = 2 \sin(p/2)$ . Results are in lattice units, with momenta given in terms of vector  $n_\mu$  of (7).

of the contraction method, for the same kinematics as in the last plot of Figure 6.

In Figure 7, there are only two points for which the contraction with momenta  $(p, q)$  gives approximately the same result as the one with vectors  $(\hat{p}, \hat{q})$ . These are the first and the last point in the graph, corresponding respectively to momentum  $p \sim (16, 0, 16)$  and  $p \sim (16, 16, 16)$ . Note that these are also the only points for which the standard and sine-adjusted reconstruction approaches exactly match, in the final plot of Figure 6: the fluctuating vertex coefficients can lead to a wrong overall reconstruction, but they cannot change an essentially correct tensor representation. With vector  $q$  being proportional to  $(16, 16, 16)$ , both special data points in the plot(s) are examples of generalised diagonal kinematics, i. e. kinematics which include either a single momentum scale  $s$  (in this case  $s = \pi$ ), or a combination of a single scale  $s$  and some vanishing momentum components. A discussion of these matters from a more analytic point of view is provided in Appendix B 1.

This brings us to the final example of such special kinematics in this paper, the symmetric configuration in three dimensions. It is given by

$$p = (-s, s, 0), \quad q = (s, 0, -s), \quad (23)$$

where  $s \equiv 2\pi n/(aN)$ , with integer  $n \in [1, N - 1]$ . For these kinematics, we shall use both the reconstruction and contraction approaches. In case of reconstruction, we do not employ the orthonormal structures of (A11), but instead turn to the manifestly Bose-symmetric ones of equation (60) in [57]. The reason for this change is simplicity. With the Bose-symmetric elements (as opposed to ON ones) it is easy to show analytically that a reduced basis can describe the continuum vertex, for kinematics of (23). One can readily verify that for a symmetric configuration (with  $p^2 = q^2 = r^2 = 2s^2$ ), the tensor  $\tau_{\mu\nu\rho}^4$  in equation (60) of [57] identically vanishes, while the element  $\tau_{\mu\nu\rho}^3$  becomes proportional to  $\tau_{\mu\nu\rho}^1$ . This leaves only the following structures:

$$\begin{aligned} \tau_{\mu\nu\rho}^1(p, q, r) &= \frac{1}{\sqrt{s^2}} \cdot [(p_\rho - q_\rho) \delta_{\mu\nu} + (q_\mu - r_\mu) \delta_{\nu\rho} + (r_\nu - p_\nu) \delta_{\rho\mu}], \\ \tau_{\mu\nu\rho}^2(p, q, r) &= \frac{1}{\sqrt{s^6}} \cdot (p_\rho - q_\rho)(q_\mu - r_\mu)(r_\nu - p_\nu). \end{aligned} \quad (24)$$

To be precise, in Landau gauge we use the fully transverse versions of the above elements, i. e. tensors that have been acted upon with the operator  $T_{\mu\alpha}^p T_{\nu\beta}^q T_{\rho\gamma}^r$ , with  $T_{\nu\beta}^q = \delta_{\nu\beta} - q_\nu q_\beta / q^2$ . The basis of (24) was also used in some previous lattice studies of the three-gluon interaction [21, 25, 26]. The element  $\tau_{\mu\nu\rho}^1$  corresponds to a tree-level structure in the continuum, and its form factor directly enters the calculations of the three-gluon running coupling. The projectors for the elements of (24) can be found easily with standard linear algebra techniques, and we shall not provide them here. We go directly to the results, displayed in Fig. 8.

On the whole, the results in the left panel of Figure 8 are better behaved than those in the lower panel of Figure 6. That is, the reconstruction results for the symmetric configuration are more in line with the analysis of

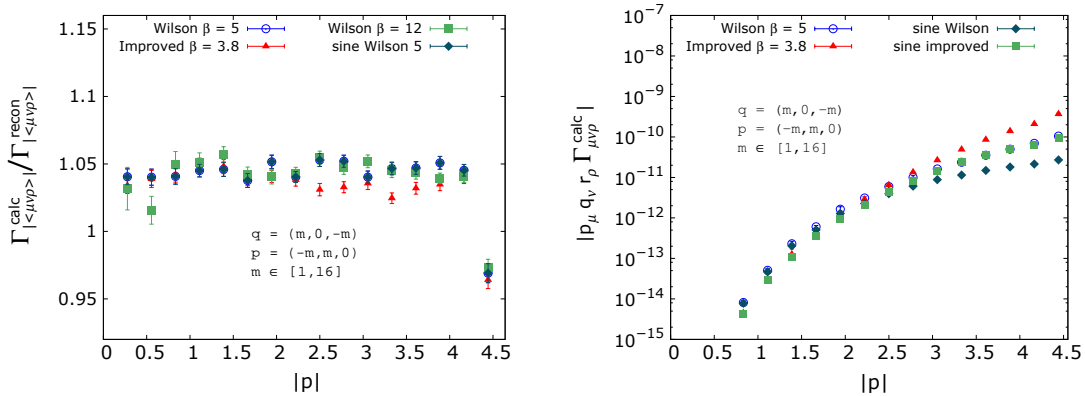


Figure 8. *Left*: Ratios of reconstructed and calculated vertices, for symmetric kinematics  $(p^2, q^2, r^2) = 2(s^2, s^2, s^2)$  on a  $32^3$  lattice. *Right*: Absolute value of contraction (21) for the same kinematics, with momenta  $(p, q)$  and their sine versions  $(\hat{p}, \hat{q})$ . Results are in lattice units, with momenta given in terms of vector  $n_\mu$  of (7).

Appendix B 1, than those in the last two plots of Figure 6. This supports our assumption that it is the number of tensors/form factors involved, that may lead to bad reconstruction results in three or higher dimensions: the symmetric configuration features only two tensors, as opposed to four elements for general 3D cases. However, some of the doubts that we pointed out to in the case of more general kinematics in three dimensions, remain true in the symmetric case. For instance, it is unclear why the original computed vertex is systematically underestimated by the reconstruction procedure, for almost all of the considered momentum points.

The above open questions notwithstanding, we do not think that the involved uncertainties significantly detract from our main message here. The main point we want to make in this paper is that the lattice three-gluon coupling can be described well with continuum tensor bases, for certain kinematics. Even with all of the associated qualms, we think that the reconstruction results of Fig. 8 support this idea nicely. This is especially fortified by the fact that we’ve considered two different gauge actions, and two different values of  $\beta$  for the Wilson action, and that in all of the examined cases the reconstructed vertex does not differ more than six percent from the calculated lattice vertex. Further, the contraction data indicate that one can indeed use the continuum momenta and tensor structures, to describe the lattice correlator with symmetric momentum partitioning (compare with Fig. 7). We note that the “growth” in the right panel of Fig. 8, as momenta  $p$  and  $q$  increase, is due to our use of the absolute value adjustment, much like in the right plot of Fig. 5.

## V. FURTHER DISCUSSION AND CONCLUDING REMARKS

In this paper we have introduced the method of vertex reconstruction as a means of checking the fidelity of various tensor representations of lattice vertex functions. We applied the method to the lattice gluon propagator and three-gluon vertex, and demonstrated that there exist special kinematic configurations for which these functions can be described in terms of continuum tensor bases. We have shown analytically why this statement holds, and provided some arguments for the application of these concepts to other primitively divergent vertex functions of QCD. We’ve also shown data which indicate that one needs to be careful when employing the vertex reconstruction procedure, as in some instances it may give misleading results. The method will likely give reliable estimates only if the involved number of vertex tensor elements is small, and if the corresponding form factors are not particularly noisy. This means that some of the lattice correlators, like the quark-gluon vertex, can almost surely not be adequately analysed with the reconstruction approach, unless a refinement or a better alternative framework is found.

Here we would like to make some additional comments on topics which are indirectly related to our results. Let us start with the diagonal kinematic configurations. One of our main conclusions in this paper is that the evaluation of vertex functions near the lattice diagonal can be advantageous due to a reduction of discretisation artifacts in vertex tensor elements. But there is yet another reason to favour the near-diagonal configurations over some generic lattice kinematics: close to the diagonal, there is also a reduction in hypercubic artifacts inherent to lattice vertex form factors. This constitutes the basis of the so-called cylindrical kinematic cut [28], where one only considers momentum configurations which are a certain (short) distance away from the diagonal. Thus, computation of lattice propagators/vertices for near-diagonal momenta can be doubly useful, as it reduces the discretisation effects in both the tensor structures and dressing functions of a given lattice correlator.

Another issue which merits a further discussion is the zero-momentum discrepancy in Figure 2. It is very likely that most of this effect comes from finite volume artifacts. But it should be mentioned that there might exist other factors which contribute at  $p = 0$ . One of the possible “culprits” is the appearance of additional tensor terms proportional to a Dirac delta function  $\delta(p)$ : it is argued in [51], by means of axiomatic field theory, that such terms may arise in tensor decompositions of gauge field propagators in both continuum and lattice theories. Besides this, on the lattice there are also tensor structures that contribute to gluon correlators at zero momentum, which have no continuum analogue and which vanish as  $a \rightarrow 0$  [29]. In order to truly assess the influence of either of these structures at vanishing lattice momentum, one would need to conduct a dedicated study with a careful consideration of finite volume and Gribov copy effects [60].

Finally, concerning the appearance of additional lattice tensors with no continuum analogue, we want to note that they might also cause the disparities we get in some of our others results, like those in Figs. 6 (bottom panel) and 8. In other words, there might exist Lorentz non-covariant elements with quantum numbers of the three-gluon vertex, which survive the constraint of (21) and which should be taken into account when constructing the vertex tensor basis [which we do not do, as we only consider continuum tensor forms that obey (21)]. We doubt that it is such terms that lead to a faulty vertex reconstruction, as these elements should be equally present in both 2D and 3D theories, in contrast to our 2D and pseudo-2D results of Figs. 4 and 6 (upper

panel), where one gets a very good vertex representation with continuum tensors alone. Future studies might be able to make a definitive claim in this regard, showing whether the discrepancies seen in some of our data are caused purely by statistical fluctuations, or by systematic lattice effects. In either case, we are looking forward to contributing to these interesting endeavours in the future.

## ACKNOWLEDGMENTS

We are grateful to R. Williams, A. Maas, A. Cucchieri, G. Eichmann and R. Alkofer for helpful discussions and a careful reading of this manuscript. TM acknowledges the partial support by CNPq. MV gratefully acknowledges the support of the Austrian science fund FWF, under Schrödinger grant J3854-N36.

### Appendix A: Vertex tensor bases in Landau gauge

#### 1. Orthonormal transverse basis

Each of the gluon legs that comprise the three-gluon interaction comes with its own momentum variable: in lattice literature, these three momenta are often denoted as  $p$ ,  $q$  and  $r$ . Due to momentum conservation at the vertex, only two of the momenta are independent. A construction principle for the three-gluon vertex basis proposed in [57] starts from the following combinations

$$k = \frac{q-p}{2}, \quad V = -r \tag{A1}$$

The first step is to orthonormalise  $k$  and  $V$  with respect to each other: this is done in a standard way as

$$d_\mu = \tilde{V}_\mu, \quad s_\mu = \tilde{k}_\mu^{tr}, \tag{A2}$$

where  $k_\mu^{tr} = T_{\mu\nu}^V k_\nu$  is a component of  $k$  transverse to  $V$ , and  $T_{\mu\nu}^V = \delta_{\mu\nu} - V_\mu V_\nu / V^2$ . Tilde ( $\tilde{\phantom{x}}$ ) in these expressions denotes a normalised vector. For purposes of later discussion we introduce the auxiliary tensors

$$\begin{aligned} \mathbb{T}_{\mu\nu}^1 &= \delta_{\mu\nu}, & \mathbb{T}_{\mu\nu}^4 &= s_\mu d_\nu + d_\mu s_\nu, \\ \mathbb{T}_{\mu\nu}^2 &= s_\mu s_\nu, & \mathbb{T}_{\mu\nu}^5 &= s_\mu d_\nu - d_\mu s_\nu. \\ \mathbb{T}_{\mu\nu}^3 &= d_\mu d_\nu, \end{aligned} \tag{A3}$$

In Landau gauge the vertex is transverse with respect to  $p$ ,  $q$  and  $r$ , or explicitly

$$p_\mu \Gamma_{\mu\nu\rho}(p, q, r) = q_\nu \Gamma_{\mu\nu\rho}(p, q, r) = r_\rho \Gamma_{\mu\nu\rho}(p, q, r) = 0. \tag{A4}$$

Thus, in Landau gauge it is sufficient to retain those linear combinations of elements in (A3) which are transverse to all of the vectors  $p$ ,  $q$  and  $r$ . It turns out that there are only 4 of them. To shorten the upcoming equations, we will use the following notation for kinematic variables

$$\begin{aligned} t &= \frac{V^2}{4}, & \eta &= \frac{4k^2}{3V^2}, & z &= \tilde{k} \cdot \tilde{V}, \\ a &= \sqrt{3\eta}z, & b &= \sqrt{3\eta}\sqrt{1-z^2}. \end{aligned} \tag{A5}$$

The above quantities are all dimensionless, except for  $t$ . The momenta  $p$ ,  $q$ ,  $r$  can now be rewritten as

$$\begin{aligned} p &= -\sqrt{t}(b s^\mu + (a-1) d^\mu), & q &= \sqrt{t}(b s^\mu + (a+1) d^\mu), \\ V &= -r = 2\sqrt{t}d. \end{aligned} \tag{A6}$$

We now need linear combinations of quantities in (A3) which have definitive transversality properties with respect to  $p$  and  $q$ . These have been constructed in [59]. Here we only provide the elements relevant for the

vertex in Landau gauge: for more general cases, consult [59] or [57]. The important objects are

$$\begin{aligned} \Upsilon_{\mu\nu}^1 &= \frac{1}{\sqrt{D-2}} (\Upsilon_{\mu\nu}^1 - \Upsilon_{\mu\nu}^2 - \Upsilon_{\mu\nu}^3), \\ \Upsilon_{\mu\nu}^2 &= \frac{1}{\sqrt{n_1 n_2}} [(1-a^2) \Upsilon_{\mu\nu}^2 - b^2 \Upsilon_{\mu\nu}^3 + ab \Upsilon_{\mu\nu}^4 - b \Upsilon_{\mu\nu}^5]. \end{aligned} \quad (\text{A7})$$

In the above expression,  $D$  denotes the number of dimensions, and we used the abbreviations

$$n_1 = 1 + a^2 + b^2, \quad n_2 = n_1 - \frac{4a^2}{n_1}. \quad (\text{A8})$$

From equations (A6) and (A7), and using the properties of  $s$  and  $d$  ( $s^2 = d^2 = 1$  and  $s \cdot d = 0$ ), it is straightforward to show that the objects  $\Upsilon_{\mu\nu}^1$  and  $\Upsilon_{\mu\nu}^2$  have the following transversality properties:

$$\begin{aligned} \Upsilon_{\mu\nu}^1 s_\mu &= \Upsilon_{\mu\nu}^1 s_\nu = \Upsilon_{\mu\nu}^1 d_\mu = \Upsilon_{\mu\nu}^1 d_\nu = 0, \\ \Upsilon_{\mu\nu}^2 p_\mu &= \Upsilon_{\mu\nu}^2 q_\nu = 0. \end{aligned} \quad (\text{A9})$$

From equations (A6) and (A9), one can see that  $\Upsilon_{\mu\nu}^1$  is transverse to all momenta  $p$ ,  $q$  and  $r$ , in both of its indices. Now, vector  $s_\mu$  is, by construction, orthogonal to  $r_\mu$ , and one thus immediately gets two fully transverse elements,  $\Upsilon_{\mu\nu}^1 s_\rho$  and  $\Upsilon_{\mu\nu}^2 s_\rho$ . The remaining objects can be obtained by taking the vector  $s$  and transversely projecting it with respect to momenta  $p$  and  $q$ , i. e.  $s_\mu^{p,q} = T_{\mu\alpha}^{p,q} s_\alpha$ . The resulting normalised momenta are

$$\begin{aligned} \tilde{s}_\mu^p &= \frac{1}{\sqrt{n_1 - 2a}} [(a-1) s_\mu - b d_\mu], \\ \tilde{s}_\mu^q &= \frac{1}{\sqrt{n_1 + 2a}} [(a+1) s_\mu - b d_\mu]. \end{aligned} \quad (\text{A10})$$

From equations (A10) and (A6) one can see that  $\tilde{s}_\mu^p$  and  $\tilde{s}_\mu^q$  are orthogonal to  $p$  and  $q$ , respectively. We now have all the ingredients to write down a complete, orthonormal and transverse basis for the Landau gauge three-gluon vertex:

$$\begin{aligned} \rho_{\mu\nu\sigma}^1 &= \Upsilon_{\mu\nu}^1 s_\sigma, & \rho_{\mu\nu\sigma}^2 &= \Upsilon_{\mu\nu}^2 s_\sigma, \\ \rho_{\mu\nu\sigma}^3 &= \Upsilon_{\sigma\nu}^1 \tilde{s}_\mu^p, & \rho_{\mu\nu\sigma}^4 &= \Upsilon_{\rho\mu}^1 \tilde{s}_\nu^q. \end{aligned} \quad (\text{A11})$$

Now let us discuss the case of two dimensions. One first notes that in 2D the vectors  $s$  and  $d$ , defined in equation (A2), take the form

$$s = \begin{pmatrix} e \\ f \end{pmatrix}, \quad d = \begin{pmatrix} f \\ -e \end{pmatrix}, \quad (\text{A12})$$

where  $f^2 + e^2 = 1$ . In two dimensions, this is the only combination that satisfies the defining characteristics of  $s$  and  $d$ , namely that  $s^2 = d^2 = 1$  and  $s \cdot d = 0$ . By plugging in the expressions of (A12) into the definition of  $\Upsilon_{\mu\nu}^1$ , component by component, one can see that the (non-normalised) version of this tensor vanishes:

$$\begin{aligned} \Upsilon_{11}^1 &= \delta_{11} - s_1 s_1 - d_1 d_1 = 1 - e^2 - f^2 = 0, \\ \Upsilon_{21}^1 &= \delta_{21} - s_2 s_1 - d_2 d_1 = fe - ef = 0, \end{aligned} \quad (\text{A13})$$

and similarly for  $\Upsilon_{12}^1$  and  $\Upsilon_{22}^1$ . The fact that  $\Upsilon_{\mu\nu}^1$  identically equals zero in 2D means that three out of four basis elements in equation (A11) also vanish, and the only surviving tensor in Landau gauge is  $\rho_{\mu\nu\sigma}^2$ . With the same kind of calculation one can show that for special kinematics in three dimensions, e. g.  $p = (m, n, 0)$  and  $q = (g, l, 0)$  (with arbitrary numbers  $m, n, g, l$ ), the structure  $\rho_{\mu\nu\sigma}^2$  will be the dominant one, as all the other elements of (A11) vanish for all but a few values of their indices  $(\mu\nu\sigma)$ . For such special 3D kinematics, the contributions of tensors  $\rho_{\mu\nu\sigma}^j$  ( $j = 1, 3, 4$ ) to the index average of (20) will be negligible, rendering the calculations essentially two-dimensional. In connection to this, one may look up the results in Figure 6 and compare the ‘‘quality’’ of data between the upper and lower panels of the Figure.

## 2. Simple Landau gauge basis

Due to the properties of orthonormality and manifest transversality, the basis given in (A7) is very useful for numerics. However, a somewhat convoluted construction can make the transverse orthonormal (ON) basis difficult to manage for analytic manipulations. In this section we describe another tensor basis for the three-gluon vertex, arguably the simplest one (in a certain sense) which one can use in Landau gauge. The upcoming analytic proofs, relevant for our study, will be carried out in full only for the Simple elements. Here we will also establish a connection between the ON and Simple bases, and it will be used to argue that all of the forthcoming results are equally well applicable to the ON structures, or indeed to any other tensor representation that one might choose to describe the three-gluon interaction.

We start the basis construction with an observation that the three-gluon coupling has two independent momentum variables (say,  $p$  and  $q$ ) and three Lorentz indices, meaning that the following 14 tensor elements should suffice to parameterise the vertex (compare Appendix A of [52]):

$$\begin{aligned} & \delta_{\mu\nu} \times \{p_\rho, q_\rho\}, \quad \delta_{\mu\rho} \times \{p_\nu, q_\nu\}, \quad \delta_{\nu\rho} \times \{p_\mu, q_\mu\}, \\ & p_\mu \times \{p_\rho p_\nu, p_\rho q_\nu, q_\rho q_\nu\}, \quad p_\nu q_\mu p_\rho, \\ & q_\mu \times \{q_\rho q_\nu, q_\rho p_\nu, p_\rho p_\nu\}, \quad q_\nu p_\mu q_\rho. \end{aligned} \quad (\text{A14})$$

Full transversality, as expressed in (A4) (with  $r = -p - q$ ) means that among the elements of (A14), one can ignore those which are proportional to components  $p_\mu$  and  $q_\nu$ . Even more than that, from momentum conservation ( $r_\rho = -p_\rho - q_\rho$ ) and the fact that the tensor  $r_\rho$  is eliminated in Landau gauge, one gets that  $p_\rho$  and  $q_\rho$  are degenerate, with  $p_\rho = -q_\rho$ . Taking into account this degeneracy and neglecting the elements proportional to  $p_\mu$  and  $q_\nu$  in (A14), one ends up with only four fully transverse elements in Landau gauge. In terms of dimensionless quantities, these tensors are

$$\begin{aligned} \sqrt{p^2} S_{\mu\nu\rho}^1 &= T_{\alpha\mu}^p T_{\beta\nu}^q T_{\gamma\rho}^r \cdot \delta_{\alpha\beta} p_\gamma, \\ \sqrt{q^2} S_{\mu\nu\rho}^2 &= T_{\alpha\mu}^p T_{\beta\nu}^q T_{\gamma\rho}^r \cdot \delta_{\beta\gamma} q_\alpha, \\ \sqrt{p^2} S_{\mu\nu\rho}^3 &= T_{\alpha\mu}^p T_{\beta\nu}^q T_{\gamma\rho}^r \cdot \delta_{\gamma\alpha} p_\beta, \\ p^2 \sqrt{q^2} S_{\mu\nu\rho}^4 &= T_{\alpha\mu}^p T_{\beta\nu}^q T_{\gamma\rho}^r \cdot q_\alpha p_\beta p_\gamma, \end{aligned} \quad (\text{A15})$$

with a transverse projector  $T_{\mu\alpha}^p = \delta_{\mu\alpha} - p_\mu p_\alpha / p^2$ , and similarly for others. The above structures are deceptively simple, since we have refrained from writing out the full expressions, with transverse projections carried out. For all of the upcoming analytic arguments, the forms given in (A15) are perfectly adequate.

The bases of (A11) and (A15) describe the same object, and thus there has to be a connection between them. In other words, there should exist a rotation operator  $R$  that effects the transformation

$$\rho_{\mu\nu\sigma}^j = \sum_{k=1}^4 R_{jk} S_{\mu\nu\sigma}^k, \quad j = 1 \dots 4. \quad (\text{A16})$$

The procedure to obtain the components of  $R$  can be broken down into a few simple steps, but we shall not provide the details here. We will just write down the non-vanishing elements of  $R$ , for a three-dimensional theory. In terms of kinematic variables  $a$ ,  $b$ ,  $t$  and  $n_1$  defined in equations (A5) and (A8), the non-zero entries of  $R$  are

$$\begin{aligned} R_{11} &= -4\sqrt{p^2}, & R_{14} &= \frac{p^2 \sqrt{q^2} (a^2 + b^2 - 1)}{b^2 t}, & R_{24} &= \frac{p^2 \sqrt{q^2}}{b^2 t n_+ n_-}, & R_{32} &= \frac{-2\sqrt{q^2}}{n_-}, \\ R_{34} &= \frac{p^2 \sqrt{q^2} (a + 1)}{b^2 t n_-}, & R_{43} &= \frac{-2\sqrt{p^2}}{n_+}, & R_{44} &= \frac{p^2 \sqrt{q^2} (a - 1)}{b^2 t n_+}, \end{aligned} \quad (\text{A17})$$

where  $n_\pm = 1/\sqrt{n_1 \pm 2a}$ . Additionally, all of the elements of  $R$  are to be divided by  $4b\sqrt{t}$ . The matrix transpose of  $R$  can be used to effect a different kind of transformation, namely to rotate the dressings functions of the ON basis (denoted  $\mathcal{B}^j$  and calculated via (19)) into the dressings of the Simple basis. We've used this fact to simultaneously perform vertex reconstructions with both ON and Simple bases, and we've checked that the two

methods give the same results. With the connection between the ON and Simple elements established via (A16), we are ready to move on with our analytic proofs.

## Appendix B: Special kinematic configurations

### 1. Generalised diagonal kinematics

In the following we wish to show that for certain kinematic configurations, the three-gluon vertex tensor representations take the same form on the lattice as they do in the continuum. In other words, we want to demonstrate that, under certain conditions, the vertex tensor elements are unaffected by the transformation

$$p_\mu \rightarrow \hat{p}_\mu, \quad (\text{B1})$$

with  $p$  being the continuum momentum and  $\hat{p}$  being its lattice-adjusted version. Following (8), which is valid for standard lattice Landau gauge implementations, we will look at a concrete example where

$$\hat{p}_\mu = 2 \sin\left(\frac{p_\mu}{2}\right). \quad (\text{B2})$$

The reader should keep in mind that most of our conclusions will actually hold for (almost) arbitrary  $\hat{p}(p)$  dependencies, as long as they obey the constraint  $\hat{p}(-p) = -\hat{p}(p)$  (which also implies  $\hat{p}(0) = 0$ ). We examine the example of symmetric kinematics in three dimensions, given by

$$p = \begin{pmatrix} n \\ -n \\ 0 \end{pmatrix}, \quad q = \begin{pmatrix} -n \\ 0 \\ n \end{pmatrix}, \quad r = \begin{pmatrix} 0 \\ n \\ -n \end{pmatrix}, \quad (\text{B3})$$

with  $n$  being a number consistent with lattice momentum discretisation. Our results will hold not just for (B3), but for any configurations that satisfy the demands that 1) the components of  $p$  and  $q$  are either  $n$  or 0, and 2) the components of  $p$  and  $q$  are organised in such a way that the lattice adjustment does not break momentum conservation. In other words, from  $r = -p - q$  it should follow that  $\hat{r} = -\hat{p} - \hat{q}$ . Besides (B3), this class of configurations would also include the 2D example of (22), and others.

One first notes that, without any loss of generality, the lattice transformation on momenta of (B3) can be written as a multiplicative factor, i. e.

$$\hat{p}_\mu = \xi \cdot p_\mu, \quad \hat{q}_\mu = \xi \cdot q_\mu, \quad \hat{r}_\mu = \xi \cdot r_\mu, \quad (\text{B4})$$

with  $\xi$  being some number. The above relation follows from the special form of the vectors in (B3): since the components of all the vectors are either  $\pm n$  or 0, they all get modified in the same way, i. e.  $\sin(n/2) = \xi \cdot n$ ,  $\sin(0) = \xi \cdot 0$ ,  $\sin(-n/2) = -\xi \cdot n$ . We shall temporarily assume that the factor  $\xi$  is strictly positive, and the possibility  $\xi < 0$  will be discussed in detail towards the end of this section. Now, one can easily see that the transverse projectors that enter the construction of Simple elements in (A15), are invariant under the scaling transformation of (B4). As an example,

$$\frac{\hat{p}_\alpha \hat{p}_\mu}{\hat{p}^2} = \frac{\xi^2 p_\alpha p_\mu}{\xi^2 p^2} = \frac{p_\alpha p_\mu}{p^2}, \quad (\text{B5})$$

and similarly for the non-trivial parts of  $T_{\beta\nu}^q$  and  $T_{\gamma\rho}^r$ . Since these operators are unaffected by the lattice adjustment, we will drop them from the definition of the Simple basis, for the derivation of the following expression. Let us see what happens with the remaining parts of the  $S_{\mu\nu\rho}^k$  structures under (B4). Concretely, let us look only at  $S_{\mu\nu\rho}^1$  and  $S_{\mu\nu\rho}^4$ , as it should be fairly obvious that the same thing happens with the other

elements as well:

$$\begin{aligned}\widehat{S}_{\mu\nu\rho}^1 &= \frac{\delta_{\mu\nu} \hat{p}_\rho}{\sqrt{\hat{p}^2}} = \frac{\xi \delta_{\mu\nu} p_\rho}{\xi \sqrt{p^2}} = \frac{\delta_{\mu\nu} p_\rho}{\sqrt{p^2}}, \\ \widehat{S}_{\mu\nu\rho}^4 &= \frac{\hat{q}_\mu \hat{p}_\nu \hat{p}_\rho}{\hat{p}^2 \sqrt{\hat{q}^2}} = \frac{\xi^3 q_\mu p_\nu p_\rho}{\xi^3 p^2 \sqrt{q^2}} = \frac{q_\mu p_\nu p_\rho}{p^2 \sqrt{q^2}}.\end{aligned}\tag{B6}$$

Thus, even with lattice-adjusted momenta, the vertex tensor structures remain the same as in the continuum. The same can be shown for other tensor representations, like the orthonormal one. From the invariance of elements  $S_{\mu\nu\sigma}^k$  and equation (A16) one can see that, to establish an absence of change for the basis  $\rho_{\mu\nu\sigma}^j$  under (B4), it should be proven that the operator  $R$  remains unaffected by lattice momentum modifications. We will not go into a detailed demonstration of this, but will outline the main steps. Combining the transformation of (B4) with definitions of (A1) and (A5) one gets:

$$\begin{aligned}\hat{t} &= \xi^2 t, & \hat{\eta} &= \eta, & \hat{z} &= z, \\ \hat{a} &= a, & \hat{b} &= b.\end{aligned}\tag{B7}$$

As one might expect, all the dimensionless quantities in (A5) remain unchanged under the rescaling of (B4). From the above results and the definition of (A8), it also follows that  $\hat{n}_1 = n_1$  and (consequently)  $\hat{n}_\pm = n_\pm$ . With this, one has all the necessary ingredients to prove the invariance of  $R$ . For instance, the lattice version of the element  $R_{44}$  would be

$$\begin{aligned}R_{44}^{\mathcal{L}} &= \hat{p}^2 \sqrt{\hat{q}^2} (\hat{a}-1)/(4\hat{b}^3 \hat{t}^{\frac{3}{2}} \hat{n}_+) = \xi^3 p^2 \sqrt{q^2} (a-1)/(\xi^3 4b^3 t^{\frac{3}{2}} n_+) = \\ &= p^2 \sqrt{q^2} (a-1)/(4b^3 t^{\frac{3}{2}} n_+) = R_{44}.\end{aligned}\tag{B8}$$

And similarly for other entries in  $R$ . Connections like the one of (A16) can be established between the Simple basis and any other appropriate tensor representations, and one would always get that the dimensionless tensor structures do not change under (B4).

Finally, we wish to comment on the case  $\xi < 0$ . While such a scenario can happen in principle, for relatively general  $\hat{p}(p)$  dependencies, it is in fact not possible in our current framework, with a periodic lattice and  $\hat{p}(p) = 2 \sin(p/2)$ . The function  $\sin(x/2)$  has the same sign as  $x$ , for all  $x \in [0, 2\pi]$ , with  $[0, 2\pi]$  being the relevant interval of values in standard lattice formulations. Thus, in our present numerical setup,  $\xi$  will always be a strictly positive factor. This fact is quite important, because it means that some of our aforementioned arguments can be applied even to kinematic configurations which resemble (B3), but which do not respect momentum conservation upon lattice adjustment, i. e.  $\hat{r} \neq -\hat{p} - \hat{q}$ . As a prime example, let us look at a diagonal situation with

$$p = \begin{pmatrix} n \\ n \\ n \end{pmatrix}, \quad q = \begin{pmatrix} n \\ n \\ n \end{pmatrix}, \quad r = -2 \begin{pmatrix} n \\ n \\ n \end{pmatrix}.\tag{B9}$$

For a configuration like the one above, the lattice modification of momenta will include two multiplicative factors, i. e.

$$\hat{p} = \xi \cdot p, \quad \hat{q} = \xi \cdot q, \quad \hat{r} = \zeta \cdot r,\tag{B10}$$

where in general  $\xi \neq \zeta$ . A potential source of problems in this case are not the numbers  $\xi, \zeta$  themselves, as their absolute values would always drop out in normalisations of vertex tensor structures, like in (B6). A possible issue lies in the fact that  $\xi$  and  $\zeta$  might have an opposite sign, with (say)  $\xi > 0$  and  $\zeta < 0$ . In such a situation, the lattice adjustment of momenta would effectively enact a transformation  $(p, q, r) \rightarrow (p, q, -r)$ , with the transformed configuration being forbidden by momentum conservation. But as we already pointed out, within our current framework this cannot happen, as both  $\xi$  and  $\zeta$  will be positive numbers. Thus, the kinematics like the one of (B9) will work just as well in our numerics, as do the ‘‘momentum-conserving’’ ones of (B3). In our data, this can be seen in the lower panel of Figure 3, as well as with the first and the last point in Figure 7.

Relative sign changes between different momenta are the reason why one should be very careful when applying these ideas to lattice correlators which include degrees of freedom other than gluons. Let us look at the example

of the quark-gluon vertex with vectors  $(p, q, r)$ , where  $p$  and  $q$  are the momenta passing through the quark legs, and  $r$  is the gluon momentum. One of the normalised vertex tensor elements would then be

$$\tau_\mu^{\text{qg}} = \frac{p_\mu \not{q}}{\sqrt{p^2 q^2}}, \quad (\text{B11})$$

where  $\not{q} = q_\mu \gamma_\mu$ , and  $\gamma_\mu$  are the Euclidean Dirac matrices. It seems obvious that for kinematic configurations like the one in (B3), the above structure would be invariant under a momentum adjustment  $(p, q) \rightarrow (\bar{p}, \bar{q})$ . Here  $\bar{p} = \zeta \cdot p$  denotes a lattice momentum transformation applicable to quark degrees of freedom, and  $\zeta$  is some number. But one ought not to forget that the gluon momentum  $r$  should also be adjusted, i. e.  $r \rightarrow \hat{r} = \xi \cdot r$ . In general, the quark and gluon momenta will be discretised differently on the lattice, and one would have  $\zeta \neq \xi$ . This includes the possibility of  $\xi$  and  $\zeta$  having an opposite sign, leading to problems with momentum conservation. Such considerations should be kept in mind when applying our scaling invariance arguments to correlators that mix different kinds of fields. But in situations where one can (somehow) guarantee that relative sign changes between different momenta cannot happen, our preceding analysis offers an useful tool to describe the tensor elements of lattice vertices with virtually no discretisation effects.

## 2. Collinear kinematics

We now wish to show that for collinear kinematic configurations, all of the tensor elements of the three-gluon vertex vanish in Landau gauge. This is the reason that, in our plots which include vertex reconstruction, we leave out the points corresponding to  $p = q$ : such a scenario is simply a special case of collinear configurations. Collinear kinematics are defined by

$$q = C_q \cdot p, \quad C_q = \text{const.} \quad (\text{B12})$$

From the above relation and momentum conservation it follows that all of the vertex vectors are multiples of a single momentum variable, which we shall take to be  $p$ :

$$p = p, \quad q = C_q \cdot p, \quad r = C_r \cdot p, \quad (\text{B13})$$

where  $C_r = -1 - C_q$ . When the relation (B13) is satisfied, the different transverse projectors of (A15) become equivalent, in a sense. As an example,

$$\frac{q_\nu q_\beta}{q^2} = \frac{C_q^2 p_\nu p_\beta}{C_q^2 p^2} = \frac{p_\nu p_\beta}{p^2}. \quad (\text{B14})$$

The same holds for the operator  $T_{\rho\gamma}^r$ , which becomes equal to  $T_{\rho\gamma}^p$ . Going back to the definitions of equation (A15), these facts entail the vanishing of all of the involved tensor structures, i. e.

$$\begin{aligned} S_{\mu\nu\rho}^1 &= T_{\alpha\mu}^p T_{\beta\nu}^p T_{\gamma\rho}^p \cdot \frac{\delta_{\alpha\beta} p_\gamma}{\sqrt{p^2}} \sim \left( \delta_{\gamma\rho} - \frac{p_\gamma p_\rho}{p^2} \right) \cdot \frac{\delta_{\alpha\beta} p_\gamma}{\sqrt{p^2}} = 0, \\ S_{\mu\nu\rho}^2 &= T_{\alpha\mu}^p T_{\beta\nu}^p T_{\gamma\rho}^p \cdot \frac{C_q \delta_{\beta\gamma} p_\alpha}{C_q \sqrt{p^2}} \sim \left( \delta_{\alpha\mu} - \frac{p_\alpha p_\mu}{p^2} \right) \cdot \frac{\delta_{\beta\gamma} p_\alpha}{\sqrt{p^2}} = 0, \\ S_{\mu\nu\rho}^3 &= T_{\alpha\mu}^p T_{\beta\nu}^p T_{\gamma\rho}^p \cdot \frac{\delta_{\gamma\alpha} p_\beta}{\sqrt{p^2}} \sim \left( \delta_{\beta\nu} - \frac{p_\beta p_\nu}{p^2} \right) \cdot \frac{\delta_{\gamma\alpha} p_\beta}{\sqrt{p^2}} = 0, \\ S_{\mu\nu\rho}^4 &= T_{\alpha\mu}^p T_{\beta\nu}^p T_{\gamma\rho}^p \cdot \frac{C_q p_\alpha p_\beta p_\gamma}{C_q p^2 \sqrt{p^2}} \sim \left( \delta_{\gamma\rho} - \frac{p_\gamma p_\rho}{p^2} \right) \cdot \frac{p_\alpha p_\beta p_\gamma}{p^2 \sqrt{p^2}} = 0. \end{aligned} \quad (\text{B15})$$

In the above expressions, we've assumed that  $C_q$  is strictly positive, since its sign makes no difference for the end result. We point out that none of these considerations apply to the case of one vanishing momentum, with either  $C_q$  or  $C_r$  being equal to zero. This is because in such a scenario (say,  $C_r = 0$ ), the corresponding transverse projector is reduced to a Kronecker delta, i. e.  $T_{\rho\gamma}^r \rightarrow \delta_{\rho\gamma}$ , meaning that some of the vertex tensor structures will survive the transverse projection.

With the vanishing of continuum Landau gauge three-gluon vertex thus established, for collinear configurations, we turn briefly to the case of the lattice correlation function. From non-linearity of the transformation (B2), it should be fairly easy to see that the conditions of (B13) will in general not survive the lattice momentum adjustment. In other words, from equation (B13) it does not follow that

$$\hat{q} = \mathcal{D}_q \cdot \hat{p}, \quad \hat{r} = \mathcal{D}_r \cdot \hat{p}, \quad (\text{B16})$$

with some constants  $\mathcal{D}_q$  and  $\mathcal{D}_r$ . Even if one chooses a configuration with  $p = q$ , so that necessarily  $\hat{p} = \hat{q}$ , one cannot keep both the condition of collinearity and the momentum conservation condition. In general, then, the lattice three-gluon correlator would not be expected to vanish, for collinear kinematic configurations.

$V$	Action	$\beta$	$a$ [GeV $^{-1}$ ]	$\langle W_{1,1} \rangle$	$(\sqrt{\sigma} a)^{\text{exp}}$	$(\sqrt{\sigma} a)^{\text{calc}}$	$\alpha^{\text{APE}}$	$\alpha^{\text{gauge}}$
$32^2$	W	10	0.93(2)	0.85432(10)	0.396	0.411(9)	0.7	0.495
$32^2$	I	8	0.95(2)	0.87441(9)	–	–	0.7	0.495
$32^3$	W	5	0.74(2)	0.78694(9)	0.313(27)	0.327(8)	0.3	0.348
$32^3$	I	3.8	0.72(2)	0.81195(9)	–	–	0.3	0.346
$32^3$	W	12	0.35(1)	0.91481(8)	0.119(14)	0.142(5)	0.3	0.324

Table I. Some details for our gauge field configurations. “W” stands for Wilson gauge action, “I” for the improved one. The value of the spacing  $a$  in GeV was set via a static  $q\bar{q}$  potential  $U_{\text{pot}}$ , with  $\sqrt{\sigma} = 0.44$  GeV. For Wilson gauge action, we provide the expected (superscript “exp”) and calculated (superscript “calc”) values for the quantity  $\sqrt{\sigma}a$ , with the expected ones coming from the analytic results of [46] (for 2D), and from a fit of equation (67) of [47] (for 3D).  $\langle W_{1,1} \rangle$  is the expectation value of the  $1 \times 1$  Wilson loop, needed for the fit in [47].  $\alpha^{\text{APE}}$  denotes the APE smearing parameter [45], used in measurements of  $U_{\text{pot}}$ .  $\alpha^{\text{gauge}}$  is the parameter for the gauge fixing procedure, the Cornell method [49].

- 
- [1] V. N. Gribov, Nucl. Phys. B **139** (1978) 1. doi:10.1016/0550-3213(78)90175-X
- [2] D. Zwanziger, Nucl. Phys. B **412** (1994) 657. doi:10.1016/0550-3213(94)90396-4
- [3] D. Zwanziger, Phys. Rev. D **65** (2002) 094039 doi:10.1103/PhysRevD.65.094039 [hep-th/0109224].
- [4] D. Zwanziger, Phys. Rev. D **69** (2004) 016002 doi:10.1103/PhysRevD.69.016002 [hep-ph/0303028].
- [5] T. Kugo and I. Ojima, Prog. Theor. Phys. Suppl. **66** (1979) 1. doi:10.1143/PTPS.66.1
- [6] M. Vujanovic and R. Williams, Eur. Phys. J. C **75** (2015) no.3, 100 doi:10.1140/epjc/s10052-015-3324-x [arXiv:1411.7619 [hep-ph]].
- [7] H. Sanchis-Alepuz and R. Williams, Phys. Lett. B **749** (2015) 592 doi:10.1016/j.physletb.2015.08.067 [arXiv:1504.07776 [hep-ph]].
- [8] D. Binosi, L. Chang, J. Papavassiliou and C. D. Roberts, Phys. Lett. B **742** (2015) 183 doi:10.1016/j.physletb.2015.01.031 [arXiv:1412.4782 [nucl-th]].
- [9] M. Mitter, J. M. Pawłowski and N. Strodthoff, Phys. Rev. D **91** (2015) 054035 doi:10.1103/PhysRevD.91.054035 [arXiv:1411.7978 [hep-ph]].
- [10] R. Williams, C. S. Fischer and W. Heupel, Phys. Rev. D **93** (2016) no.3, 034026 doi:10.1103/PhysRevD.93.034026 [arXiv:1512.00455 [hep-ph]].
- [11] A. K. Cyrol, M. Mitter, J. M. Pawłowski and N. Strodthoff, arXiv:1706.06326 [hep-ph].
- [12] J. Rodriguez-Quintero, D. Binosi, C. Mezrag, J. Papavassiliou and C. D. Roberts, arXiv:1801.10164 [nucl-th].
- [13] C. D. Roberts and A. G. Williams, Prog. Part. Nucl. Phys. **33** (1994) 477 [hep-ph/9403224].
- [14] R. Alkofer and L. von Smekal, Phys. Rept. **353** (2001) 281 [hep-ph/0007355].
- [15] I. C. Cloet and C. D. Roberts, Prog. Part. Nucl. Phys. **77** (2014) 1 [arXiv:1310.2651 [nucl-th]].
- [16] G. Eichmann, H. Sanchis-Alepuz, R. Williams, R. Alkofer and C. S. Fischer, Prog. Part. Nucl. Phys. **91** (2016) 1 doi:10.1016/j.pnpnp.2016.07.001 [arXiv:1606.09602 [hep-ph]].
- [17] J. M. Pawłowski, M. M. Scherer, R. Schmidt and S. J. Wetzel, Annals Phys. **384** (2017) 165 doi:10.1016/j.aop.2017.06.017 [arXiv:1512.03598 [hep-th]].
- [18] A. Maas, Phys. Rept. **524** (2013) 203 doi:10.1016/j.physrep.2012.11.002 [arXiv:1106.3942 [hep-ph]].
- [19] C. Parrinello, Phys. Rev. D **50** (1994) R4247 doi:10.1103/PhysRevD.50.R4247 [hep-lat/9405024].
- [20] B. Alles, D. Henty, H. Panagopoulos, C. Parrinello, C. Pittori and D. G. Richards, Nucl. Phys. B **502** (1997) 325 doi:10.1016/S0550-3213(97)00483-5 [hep-lat/9605033].

- [21] P. Boucaud, J. P. Leroy, J. Micheli, O. Pene and C. Roiesnel, JHEP **9810** (1998) 017 doi:10.1088/1126-6708/1998/10/017 [hep-ph/9810322].
- [22] J. Skullerud and A. Kizilersu, JHEP **0209** (2002) 013 doi:10.1088/1126-6708/2002/09/013 [hep-ph/0205318].
- [23] J. I. Skullerud, P. O. Bowman, A. Kizilersu, D. B. Leinweber and A. G. Williams, JHEP **0304** (2003) 047 doi:10.1088/1126-6708/2003/04/047 [hep-ph/0303176].
- [24] P. Boucaud, M. Brinet, F. De Soto, V. Morenas, O. Pène, K. Petrov and J. Rodriguez-Quintero, JHEP **1404** (2014) 086 doi:10.1007/JHEP04(2014)086 [arXiv:1310.4087 [hep-ph]].
- [25] A. Athenodorou, D. Binosi, P. Boucaud, F. De Soto, J. Papavassiliou, J. Rodriguez-Quintero and S. Zafeiropoulos, Phys. Lett. B **761** (2016) 444 doi:10.1016/j.physletb.2016.08.065 [arXiv:1607.01278 [hep-ph]].
- [26] P. Boucaud, F. De Soto, J. Rodriguez-Quintero and S. Zafeiropoulos, Phys. Rev. D **95** (2017) no.11, 114503 doi:10.1103/PhysRevD.95.114503 [arXiv:1701.07390 [hep-lat]].
- [27] A. Sternbeck, P. H. Balduf, A. Kizilersu, O. Oliveira, P. J. Silva, J. I. Skullerud and A. G. Williams, PoS LATTICE **2016** (2017) 349 doi:10.22323/1.256.0349 [arXiv:1702.00612 [hep-lat]].
- [28] D. B. Leinweber *et al.* [UKQCD Collaboration], Phys. Rev. D **60** (1999) 094507 Erratum: [Phys. Rev. D **61** (2000) 079901] doi:10.1103/PhysRevD.61.079901, 10.1103/PhysRevD.60.094507 [hep-lat/9811027].
- [29] H. J. Rothe, World Sci. Lect. Notes Phys. **43** (1992) 1 [World Sci. Lect. Notes Phys. **59** (1997) 1] [World Sci. Lect. Notes Phys. **74** (2005) 1] [World Sci. Lect. Notes Phys. **82** (2012) 1].
- [30] A. Cucchieri, T. Mendes and A. Mihara, JHEP **0412** (2004) 012 doi:10.1088/1126-6708/2004/12/012 [hep-lat/0408034].
- [31] A. Cucchieri, A. Maas and T. Mendes, Phys. Rev. D **74** (2006) 014503 doi:10.1103/PhysRevD.74.014503 [hep-lat/0605011].
- [32] A. Maas, Phys. Rev. D **75** (2007) 116004 doi:10.1103/PhysRevD.75.116004 [arXiv:0704.0722 [hep-lat]].
- [33] A. Cucchieri, A. Maas and T. Mendes, Phys. Rev. D **77** (2008) 094510 doi:10.1103/PhysRevD.77.094510 [arXiv:0803.1798 [hep-lat]].
- [34] J. C. R. Bloch, A. Cucchieri, K. Langfeld and T. Mendes, Nucl. Phys. B **687** (2004) 76 doi:10.1016/j.nuclphysb.2004.03.021 [hep-lat/0312036].
- [35] B. Blossier *et al.*, Phys. Rev. Lett. **108** (2012) 262002 doi:10.1103/PhysRevLett.108.262002 [arXiv:1201.5770 [hep-ph]].
- [36] B. Blossier *et al.* [ETM Collaboration], Phys. Rev. D **89** (2014) no.1, 014507 doi:10.1103/PhysRevD.89.014507 [arXiv:1310.3763 [hep-ph]].
- [37] B. Blossier, P. Boucaud, M. Brinet, F. De Soto, V. Morenas, O. Pène, K. Petrov and J. Rodríguez-Quintero, Phys. Rev. D **89** (2014) no.3, 034026 doi:10.1103/PhysRevD.89.034026 [arXiv:1312.1514 [hep-lat]].
- [38] K. G. Wilson, Phys. Rev. D **10**, 2445 (1974). doi:10.1103/PhysRevD.10.2445
- [39] K. Symanzik, Nucl. Phys. B **226** (1983) 187. doi:10.1016/0550-3213(83)90468-6
- [40] K. Symanzik, Nucl. Phys. B **226** (1983) 205. doi:10.1016/0550-3213(83)90469-8
- [41] P. Weisz, Nucl. Phys. B **212** (1983) 1. doi:10.1016/0550-3213(83)90595-3
- [42] P. Weisz and R. Wohlert, Nucl. Phys. B **236** (1984) 397 Erratum: [Nucl. Phys. B **247** (1984) 544]. doi:10.1016/0550-3213(84)90563-7, 10.1016/0550-3213(84)90543-1
- [43] M. Luscher and P. Weisz, Commun. Math. Phys. **97** (1985) 59 Erratum: [Commun. Math. Phys. **98** (1985) 433]. doi:10.1007/BF01206178
- [44] U. Wolff [ALPHA Collaboration], Comput. Phys. Commun. **156** (2004) 143 Erratum: [Comput. Phys. Commun. **176** (2007) 383] doi:10.1016/S0010-4655(03)00467-3, 10.1016/j.cpc.2006.12.001 [hep-lat/0306017].
- [45] M. Albanese *et al.* [APE Collaboration], Phys. Lett. B **192** (1987) 163. doi:10.1016/0370-2693(87)91160-9
- [46] H. G. Dosch and V. F. Muller, Fortsch. Phys. **27** (1979) 547. doi:10.1002/prop.19790271103
- [47] M. J. Teper, Phys. Rev. D **59** (1999) 014512 doi:10.1103/PhysRevD.59.014512 [hep-lat/9804008].
- [48] K. G. Wilson, NATO Sci. Ser. B **59** (1980) 363. doi:10.1007/978-1-4684-7571-5-20
- [49] C. T. H. Davies, G. G. Batrouni, G. R. Katz, A. S. Kronfeld, G. P. Lepage, K. G. Wilson, P. Rossi and B. Svetitsky, Phys. Rev. D **37** (1988) 1581. doi:10.1103/PhysRevD.37.1581
- [50] A. Cucchieri and T. Mendes, Nucl. Phys. B **471** (1996) 263 doi:10.1016/0550-3213(96)00177-0 [hep-lat/9511020].
- [51] P. Lowdon, Phys. Rev. D **96** (2017) no.6, 065013 doi:10.1103/PhysRevD.96.065013 [arXiv:1702.02954 [hep-th]].
- [52] A. I. Davydychev, P. Osland and O. V. Tarasov, Phys. Rev. D **54** (1996) 4087 Erratum: [Phys. Rev. D **59** (1999) 109901] doi:10.1103/PhysRevD.59.109901, 10.1103/PhysRevD.54.4087 [hep-ph/9605348].
- [53] A. I. Davydychev, P. Osland and O. V. Tarasov, Phys. Rev. D **58** (1998) 036007 doi:10.1103/PhysRevD.58.036007 [hep-ph/9801380].
- [54] M. Binger and S. J. Brodsky, Phys. Rev. D **74** (2006) 054016 doi:10.1103/PhysRevD.74.054016 [hep-ph/0602199].
- [55] N. V. Smolyakov, Theor. Math. Phys. **50** (1982) 225 [Teor. Mat. Fiz. **50** (1982) 344]. doi:10.1007/BF01016449
- [56] A. L. Blum, R. Alkofer, M. Q. Huber and A. Windisch, Acta Phys. Polon. Supp. **8** (2015) no.2, 321 doi:10.5506/APhysPolBSupp.8.321 [arXiv:1506.04275 [hep-ph]].
- [57] G. Eichmann, R. Williams, R. Alkofer and M. Vujanovic, Phys. Rev. D **89** (2014) no.10, 105014 doi:10.1103/PhysRevD.89.105014 [arXiv:1402.1365 [hep-ph]].
- [58] A. Cucchieri, Phys. Rev. D **60** (1999) 034508 doi:10.1103/PhysRevD.60.034508 [hep-lat/9902023].
- [59] G. Eichmann and C. S. Fischer, Phys. Rev. D **87** (2013) no.3, 036006 doi:10.1103/PhysRevD.87.036006 [arXiv:1212.1761 [hep-ph]].
- [60] A. Cucchieri, Nucl. Phys. B **508** (1997) 353 doi:10.1016/S0550-3213(97)80016-8, 10.1016/S0550-3213(97)00629-9

[hep-lat/9705005].